JACC: CASE REPORTS VOL. 29, 2024
PUBLISHED BY ELSEVIER ON BEHALF OF THE AMERICAN COLLEGE OF CARDIOLOGY FOUNDATION.

IMAGING VIGNETTE

CLINICAL VIGNETTE

Multimodal Imaging Findings Associated With Cardiac Oxalosis Cardiomyopathy

Murtaza Ali, MD,[a] Gohar Rundhawa, MD,[a] C. Anwar A. Chahal, MD,[b,c] Rahul Kashyap, MD,[d] Joseph J. Maleszewski, MD,[e,f,g] Ron Jacob, MD,[b] Drew Ertel, MD,[b] Michael N. Vranian, MD[b]

ABSTRACT

We report the case of a 50-year-old woman with secondary oxalosis following bowel resection resulting in restrictive cardiomyopathy and a diagnosis of cardiac amyloidosis based on the initial workup. The case documented findings by cardiac magnetic resonance imaging and technetium Tc 99m–labeled pyrophosphate scan in patients with cardiac oxalosis, which can mimic findings in cardiac amyloidosis, expanding the differential diagnosis. (J Am Coll Cardiol Case Rep 2024;29:102148) Published by Elsevier on behalf of the American College of Cardiology Foundation. This is an open access article under the CC BY-NC-ND license (http://creativecommons.org/licenses/by-nc-nd/4.0/).

Primary oxalosis is a disorder characterized by increased production of oxalic acid due to enzymatic deficiencies. There are 3 types of primary hyperoxaluria caused by deficiencies in *AGXT*, *GRHPR*, or *HOGA1*, respectively. Secondary hyperoxaluria is caused by increased ingestion of oxalate, oxalate precursors, or altered intestinal microflora.[1]

In enteric hyperoxaluria, fat malabsorption causes undigested fatty acids to combine with calcium, resulting in increased oxalate absorption. When glomerular filtration rate falls below 30-40 mL/min/1.73 m^2, plasma oxalate levels increase promoting calcium oxalate crystallization and systemic deposition including the heart.[2,3]

A 49-year-old woman with end-stage renal disease secondary to nephrocalcinosis was hospitalized for heart failure. Initial vitals were unremarkable, and physical exam was significant for bilateral carpal tunnel, pulmonary crackles, and lower extremity edema. Lab results showed white blood cells 13 K/μL, hemoglobin 11.6 g/dL, platelets 311 K/μL, sodium 136 mmol/L, aspartate aminotransferase 38 IU/L, alanine transaminase 34 IU/L, total bilirubin 0.4 mg/dL, blood urea nitrogen 30 mg/dL, creatinine 7.12 mg/dL, glomerular filtration rate 7 mL/min/1.73 m^2, troponin I 0.25 ng/mL, and B-type natriuretic peptide 1,717 pg/mL. κ/λ free light chain ratio was normal. A 12-lead electrocardiogram exhibited sinus rhythm with nonspecific T-wave changes and low QRS voltage in the limb leads (**Figure 1**). A transthoracic echocardiogram revealed an increased left ventricular wall thickness with diastolic parameters and left atrial enlargement suggestive of a restrictive cardiomyopathy (**Figure 1**). Given the low QRS voltage, carpal tunnel syndrome, and transthoracic echocardiogram findings, an infiltrative process, specifically amyloidosis, was suspected. Cardiac magnetic resonance

From the [a]Department of Internal Medicine, York Hospital, WellSpan Health, York, Pennsylvania, USA; [b]Department of Cardiology, York Hospital, WellSpan Health, York, Pennsylvania, USA; [c]Department of Inherited Cardiovascular Diseases, WellSpan Health, Lancaster, Pennsylvania, USA; [d]Department of Research, York Hospital, WellSpan Health, York, Pennsylvania, USA; [e]Department of Laboratory Medicine and Pathology, Mayo Clinic, Rochester, Minnesota, USA; [f]Department of Cardiovascular Medicine, Mayo Clinic, Rochester, Minnesota, USA; and the [g]Department of Medical Genomics, Mayo Clinic, Rochester, Minnesota, USA.

The authors attest they are in compliance with human studies committees and animal welfare regulations of the authors' institutions and Food and Drug Administration guidelines, including patient consent where appropriate. For more information, visit the Author Center.

Manuscript received September 21, 2023; revised manuscript received October 31, 2023, accepted November 2, 2023.

ISSN 2666-0849 https://doi.org/10.1016/j.jaccas.2023.102148

demonstrated normal left ventricular size with borderline left ventricular hypertrophy and mildly reduced systolic function (ejection fraction 45%). There was diffuse circumferential late gadolinium enhancement of the left ventricle with altered gadolinium kinetics suggestive of an infiltrative process (Supplemental Figure 1). Technetium Tc 99m-labeled pyrophosphate scan demonstrated mild diffuse uptake in the left ventricular myocardium with a semi-quantitative score of 1 and a heart-to-contralateral lung ratio of 1.5 (Supplemental Figure 2). The patient underwent a fat pad biopsy that was negative with negative Congo red staining. A ventricular endomyocardial biopsy was performed that revealed moderate myocyte hypertrophy with mild interstitial (pericellular-type) fibrosis. No amyloidosis, myocarditis, or granulomas were observed. Scattered intramyocardial birefringent crystals were identified within the myocardium, which were morphologically consistent with oxalate deposition, leading to a diagnosis of myocardial oxalosis (Supplemental Figure 3). Genetic studies were performed to evaluate for known restrictive, hypertrophic, and nonischemic cardiomyopathies, including hereditary transthyretin, which were all negative. Genetic testing for primary hyperoxalosis was negative with only wild-type alleles detected for *AGXT*, *GRHPR*, or *HOGA1*. A diagnosis of secondary oxalosis (enteric type) due to bowel resection was made. This case demonstrates an overlap in imaging findings between cardiac amyloidosis and oxalosis.

FUNDING SUPPORT AND AUTHOR DISCLOSURES

The authors have reported that they have no relationships relevant to the contents of this paper to disclose.

ADDRESS FOR CORRESPONDENCE: Dr Murtaza Ali, WellSpan York Hospital, 8401 Governor Bradford Lane, Ellicott City, Maryland 21043, USA. E-mail: mali2@wellspan.org.

FIGURE 1 ECG and TTE

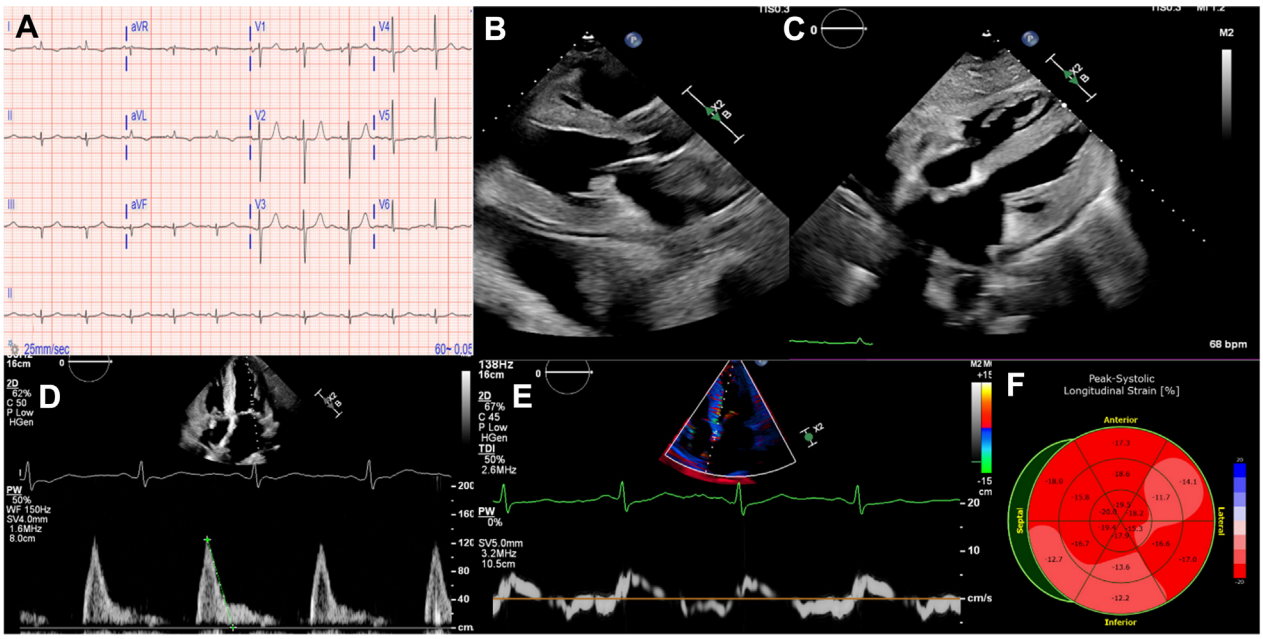

(A) Electrocardiogram (ECG) sinus rhythm with nonspecific T-wave changes and low voltage in the limb leads and poor R-wave progression in precordial leads. (B) Parasternal long-axis view on echocardiogram. Increased thickness of the left ventricular septum and posterior wall. (C) Subcostal 4-chamber view on echocardiogram demonstrating increased left and right ventricular thickness and increased thickness of the interatrial septum. (D) Mitral inflow displaying a restrictive filling pattern. (E) Low tissue annular Doppler displaying intrinsic myocardial disease. (F) Strain plot demonstrating a decrease in strain values with a global left ventricular longitudinal strain value of −16. TTE = transthoracic echocardiogram.

REFERENCES

1. Bhasin B, Ürekli HM, Atta MG. Primary and secondary hyperoxaluria: understanding the enigma. *World J Nephrol*. 2015;4(2):235-244. https://doi.org/10.5527/wjn.v4.i2.235

2. Lee DH, Kasprowicz T, Morales A, Sotolongo I, Fernandez J, Korabathina R. A case of infiltrative cardiomyopathy secondary to primary hyperoxaluria type 2—utilization of multimodality imaging. *Cureus*. 2021;13(9):e17914. https://doi.org/10.7759/cureus.17914

3. Witting C, Langman CB, Assimos D, et al. Pathophysiology and treatment of enteric hyperoxaluria. *Clin J Am Soc Nephrol*. 2021;16(3):487-495. https://doi.org/10.2215/CJN.08000520

KEY WORDS amyloidosis, calcium oxalosis, cardiac magnetic resonance, hyperoxaluria, pathology, restrictive cardiomyopathy, technetium pyrophosphate

APPENDIX For supplemental figures, please see the online version of this paper.